

DEPENDENCE OF UNSTEADY HEAT TRANSFER ON HEAT FLUX DENSITY

E. V. Kudryavtsev and I. A. Turchin

Inzhenerno-Fizicheskii Zhurnal, Vol. 10, No. 5, pp. 573-576, 1966

UDC 536.25

With the aid of an interferometer, the dependence of heat transfer coefficient in unsteady heat transfer on the rate of change of thermal stress at the heat transfer surface has been determined.

In the case of unsteady heat transfer under identical hydrodynamic conditions, the heat transfer coefficient depends on the physical properties and dimensions of the heated (or cooled) body or the wall; in other words, at times corresponding to the same temperature head (i. e., the same difference between the temperature of the wall and that of the medium at infinity), different heated bodies must receive different amounts of heat, or the heat transfer coefficient must be different. In [1] a direct presentation of the above-mentioned dependence of heat transfer coefficients on the material and the body dimensions for unsteady heat transfer was given, but the mechanism of the process remained unexplained. It was necessary to convince oneself of the rearrangement of the thermal boundary layer in unsteady heat transfer and show its appreciable difference for different bodies at the same temperature head. In this situation it was natural, in order to generalize the problem, to replace the influence of the physical parameters and dimensions of the body by the different rate of thermal potential at the wall. With this object, a thin nichrome ribbon was used as the heated (or cooled) body, its electrical heating being capable of variation over sufficiently wide limits, and the corresponding formation of the thermal boundary layer could be directly controlled with the aid of an interferometer.

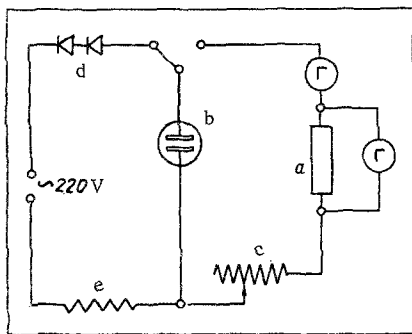


Fig. 1. Experimental circuit.

The basic element of the equipment (Fig. 1) was a nichrome ribbon *a* of dimensions $157 \times 20 \times 7 \cdot 10^{-3}$ mm. The ribbon was stretched between two copper prisms acting as current terminals, and was positioned in the field of an IZK-454 interferometer, along the beam, in the vertical plane.

Thus, the hydrodynamic process was determined by natural convection on both sides of the ribbon. The

system included electric capacitors *b* of capacity $5000 \mu\text{F}$, and a variable resistor *c*, which allowed the rate of discharge of the capacitors to be controlled, and hence the rate of change of the thermal potential.

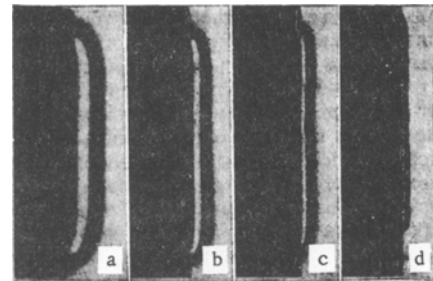


Fig. 2. Temperature field at the isotherms (interferograms) around the heated ribbon for $T_w - T_s = 7^\circ$: a) with $\tau = 0.417$ sec; b) 0.125; c) 0.042; d) 0.021.

The capacitors were charged from a 220-volt ac circuit through two series D-207 diodes *d*, and wire-wound 12-ohm resistor *e*.

During the experiments measurements were made of the air temperature and pressure, and of ribbon current and voltage, the variation of which with time was recorded on a N-105 oscillograph with provision for a simultaneous photography of the interferometer picture. The temperatures of the ribbon surface in the boundary layer were determined with the aid of the interferometer according to the method described in [2].

The ribbon heating process, which occurred in a fraction of a second, was photographed at a rate of 48 frames per second on 35 mm A-2 type film.

The identity of the experimental conditions ensured that all variations of the power slope were confined to a short time interval. Four variants of the process were chosen for reducing the data, the experimental material being processed as follows.

For each of the four variants, with different energy intensities supplied to the ribbon, an interferogram was found with the same ribbon surface temperature (Fig. 2). The temperatures of the surface and of the boundary layer were determined from the interferograms. From these data graphs were constructed for comparing one variant with another (Fig. 3). The amount of heat given out by the ribbon, and the time from the instant of completing the capacitor circuit to the establishment of an assigned temperature head were calculated for each curve.

Figure 3a shows the temperature profiles of the

boundary layer for the four variants of energy supply to the ribbon, at the time when it reached a temperature of 30.3°C , i. e., a temperature head of $\Delta t = 7^{\circ}$; for Fig. 3b the value is $\Delta t = 16.8^{\circ}$.

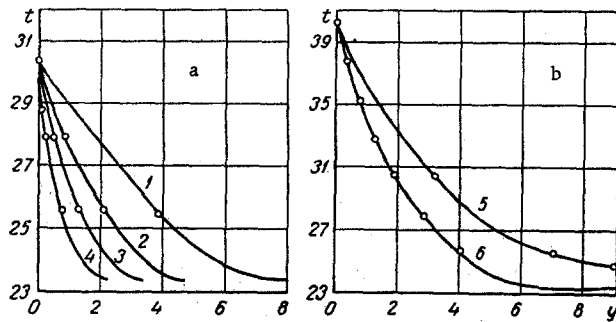


Fig. 3. Temperature profiles (t in $^{\circ}\text{C}$, y in mm) for unsteady heating of a nichrome ribbon for $T_w - T_s = 7^{\circ}$ (a) and 16.8° (b): 1) with $Q = 0.8 \text{ j}$ and $\tau = 0.417 \text{ sec}$; 2) 0.57 and 0.125; 3) 0.44 and 0.042; 4) 0.36 and 0.010; 5) 0.91 and 0.52; 6) 0.73 and 0.167.

From analysis of Figs. 2 and 3a, which show the test results for four conditions with the same $\Delta t = 7^{\circ}$, it follows that different boundary layer thicknesses and different temperature profiles correspond to the different heating rates; as a result, different heat fluxes occur for equal temperature heads.

We must evidently compare this with the case of walls of identical material, but of different thickness, when the heating (or cooling) temperature, under identical conditions, is greater for a thin wall, which corresponds to greater curvature of the temperature profile in the boundary layer; the heat transfer coefficient will then be altered in the reverse sense, i. e., the larger slope of heat flux will correspond to a smaller value of the heat transfer coefficient, and vice versa.

It is interesting to check the test results according to the Fourier law and according to the energy conservation law (heat balance). In the first case the temperature gradient was determined directly from the interferograms, while the thermal conductivity of air was taken from tables; in the second case, the amount of heat liberated in the ribbon was compared with the enthalpy of the boundary layer, allowing for two corrections—the heat capacity of the ribbon itself (of the order of 20%), and radiation (0.1%). In both cases quite favorable results were obtained, which

testifies to the accuracy of the experiments and to the reliability of the main conclusions.

In conclusion, attention should be drawn to Fig. 4, which presents interferograms of the nichrome ribbon for three different heating conditions in the course of equal time intervals of 0.417 sec after completion of the circuit. In these photographs the heating process is characterized by the isotherms located around the ribbon. It is clear from the figure that the temperature of the ribbon surface and the temperature distribution in the boundary layer at the end of the time interval in question are different. The highest surface temperature (49°C) corresponds to the maximum ribbon heating rate, and vice versa.

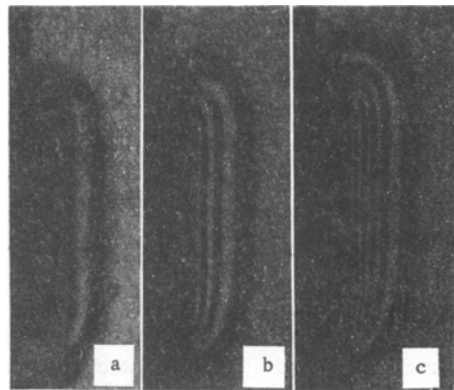


Fig. 4. Temperature field and isotherms around the heated nichrome ribbon for $\tau = 0.417 \text{ sec}$: a) with $t = 30.3^{\circ}\text{C}$; b) 37.8 ; c) 49 .

NOTATION

T —temperature; τ —time; Q —amount of heat; $\Delta t = T_w - T_s$.
Subscripts: w —values at wall; s —at infinity.

REFERENCES

1. E. V. Kudryavtsev, K. N. Chakalov, and N. V. Shumakov, Unsteady Heat Transfer [in Russian], Izd. AN SSSR, 1961.
2. V. V. Malozemov and I. A. Turchin, IFZh [Journal of Engineering Physics], 8, no. 2, 1965.

20 December 1965

Moscow Institute of Building Physics